A fast inverse solver for the filtration function for flow of water with particles in porous media

2006 Inverse Problems 22 69

(http://iopscience.iop.org/0266-5611/22/1/005)

INSTITUTE OF PHYSICS PUBLISHING INVERSE PROBLEMS

Inverse Problems **22** (2006) 69–88 doi:10.1088/0266-5611/22/1/005

A fast inverse solver for the filtration function for flow of water with particles in porous media

A C Alvarez[1,2], P G Bedrikovetsky[3], G Hime[1,4], A O Marchesin[5], D Marchesin[1] and J R Rodrigues[6]

[1] National Institute for Pure and Applied Mathematics (IMPA), Estrada Dona Castorina 110, Rio de Janeiro, RJ 22460-320, Brazil
[2] Oceanography Institute, CITMA, Avenida Primea, 18406, Flores, Playa, C. Havana, Cuba
[3] Petroleum Engineering and Exploration Laboratory (LENEP), Universidade Estadual Norte Fluminense (UENF), Rua Sebastião Lopes da Siva 56, Macaé, RJ 27937-150, Brazil
[4] National Laboratory of Scientific Computing (LNCC), Avenida Getúlio Vargas, 333, Quitandinha, Petŕopolis, RJ 25651-075, Brazil
[5] ARUP, 155 Avenue of the Americas, New York, NY 100 13, USA
[6] CENPES, Petrobras, Cidade Universitária, Quadra 7, Ilha do Fundão, Rio de Janeiro, RJ, Brazil

E-mail: meissa98@fluid.impa.br, pavel@lenep.uenf.br, hime@fluid.impa.br, andrew.marchesin@arup.com, marchesi@fluid.impa.br and jrrodrigues@petrobras.br

Received 14 July 2005, in final form 8 November 2005
Published 22 December 2005
Online at stacks.iop.org/IP/22/69

Abstract

Models for deep bed filtration in the injection of seawater with solid inclusions depend on an empirical filtration function that represents the rate of particle retention. This function must be calculated indirectly from experimental measurements of other quantities. The practical petroleum engineering purpose is to predict injectivity loss in the porous rock around wells. In this work, we determine the filtration function from the effluent particle concentration history measured in laboratory tests knowing the inlet particle concentration. The recovery procedure is based on solving a functional equation derived from the model equations. Well-posedness of the numerical procedure is discussed. Numerical results are shown.

1. Introduction

Most of the oil in the world is produced by injecting water in some wells and recovering oil in other wells. The recovered oil comes with reservoir water, which contains oil droplets and solid particles. The produced water must be separated from the oil and discarded taking environmental precautions. In offshore fields, produced water and seawater are injected. However, the injection of poor quality water in a well curtails its injectivity because the particles suspended in the fluid are trapped while passing through the porous rock. This is due to particle retention in the pores or *deep bed filtration*. In this paper, we study the deep bed

filtration during injection of water containing solid particles, which is essential to predict the loss of injectivity in wells.

Many laboratory studies were carried out to understand the filtration process [7, 8]. Our work utilizes the model for deep bed filtration developed in [2] based on the fundamental work of Hertzig *et al* [8], which consists of equations expressing the particle mass conservation and the particle retention process [3, 8, 14]. They form a quasi-linear hyperbolic system of equations containing the empirical *filtration function* $\lambda(\sigma)$, which represents the kinetics of particle retention.

Methods for determining the filtration function from the effluent concentration history at the core outlet $c_e(T)$ were presented in [15, 18], for constant filtration λ. A recovery method for the general case was presented in [4, 2], under the assumption that the injected particle concentration is constant.

In this work, a method for obtaining the filtration function is studied relaxing the assumption made in [4] of constant injected particle concentration. The inverse problem consists of determining $\lambda(\sigma)$ from the outlet and inlet particle concentration histories $c_e(T)$ and $c_i(T)$. The recovery method reduces to solving a functional equation, which is derived from an invariant along the characteristic lines. The effluent concentration history $c_e(T)$ is measured in laboratory experiments. Because of cake formation, $c_i(T)$ is smaller than the particle concentration in the fluid used in the injection experiment. This cake consists of particles that do not succeed in penetrating the wall where fluid is injected.

The paper is organized as follows. In section 2, we present the deep bed filtration model as a quasi-linear system of hyperbolic equations. Existence, uniqueness and continuous dependence on the initial and boundary conditions are discussed. In section 3, the inverse problem solved in this work is presented, transformed into a functional equation. We prove that this equation has a unique solution that depends on the given data in a weakly continuous way. In section 4, regularity of the numerical solution is discussed. In section 5, the numerical results are shown. Our conclusions are summarized in section 6. Proofs of regularity of the solution of the inverse problem and well-posedness of our numerical procedure for finding the solutions are found in the appendix.

2. Global solution for the direct problem in one dimension

We assume that water is incompressible and that the mass density of solid particles is equal in both suspended and entrapped states. Neglecting diffusive effects, the conservation of total flux is given by

$$\operatorname{div} \hat{u} = 0,$$

and the particle mass balance [2, 7] can be written as

$$\frac{\partial}{\partial t}(\phi \hat{c} + \hat{\sigma}) + \nabla(\hat{u}\hat{c}) = 0, \tag{2.1}$$

where $\hat{u}$ is the flow velocity, $\hat{c}$ and $\hat{\sigma}$ are the suspended and deposited concentrations, respectively, and ϕ is the porosity of the medium. The quantity $\hat{c}$ takes values in the $[0, 1]$ range, while $\hat{\sigma}$ takes values in the $[0, \phi)$ range.

We are interested in one-dimensional flow along the x-direction, in a laboratory sample. In this case, $\hat{u}(t)$ is the injection rate of the fluid, which is measured in the experiments; in fact, it is usually kept constant.

The model [2, 8] requires a law for particle deposition rate:

$$\frac{\partial \hat{\sigma}}{\partial t} = \hat{\Lambda}.$$

The form of $\hat{\Lambda}$ is not known from first principles: following [9, 8], we take it as

$$\hat{\Lambda}(\hat{\sigma}, \hat{u}, \hat{c}) = \hat{\lambda}(\hat{\sigma})\hat{u}\hat{c}. \tag{2.2}$$

The right-hand side of equation (2.2) means that the retention probability is proportional to the available concentration of suspended particles. This concentration is in turn proportional to $\hat{c}$ and to the flow velocity $\hat{u}$. Physically, equation (2.2) cannot be valid for large $\hat{c}$ or $\hat{\sigma}$; in particular, it cannot take into account the release of deposited particles. The positive $\hat{\lambda}(\hat{\sigma})$ is an empirical coefficient known as the *filtration function*, which cannot be measured directly.

Throughout the rest of the paper, we will use a non-dimensional form of the expressions above, introducing the following change of variables:

$$X = \frac{x}{L}, \qquad \frac{\mathrm{d}T}{\mathrm{d}t} = \frac{\hat{u}}{\phi L}, \qquad c = \hat{c}, \qquad \sigma = \frac{\hat{\sigma}}{\phi}. \tag{2.3}$$

Here, L is the length of the physical domain, so $X \in [0, 1]$, and σ is the saturation of the porous volume, so $\sigma \in [0, 1]$ as well. This allows us to write the equation (2.1) for linear flow in non-dimensional form as

$$\frac{\partial}{\partial T}(c + \sigma) + \frac{\partial c}{\partial X} = 0. \tag{2.4}$$

The unknowns $c(X, T)$ and $\sigma(X, T)$ are defined at position X and time T. The time T is in a non-dimensional unit called pore volume or PV and takes non-negative values. Moreover, usually $c \cong 10^{-4}$.

In non-dimensional form, Equation (2.2) becomes

$$\frac{\partial \sigma}{\partial T} = \lambda(\sigma)c. \tag{2.5}$$

The right-hand side of (2.5) is the non-dimensional form $\Lambda(\sigma, c)$ of $\hat{\Lambda}$. Note that the velocity $\hat{u}(t)$ has been scaled out of the equations with the change of variables (2.3). This means that the non-dimensional equations are applicable irrespectively of the injection rate dependence on time. Accordingly, from this point on the variable u does not occur in the equations.

2.1. Boundary and initial conditions

We assume that the solid particle concentration entering the porous medium is given, i.e.,

$$X = 0: \qquad c(0, T) = c_i(T) > 0, \qquad T > 0. \tag{2.6}$$

As initial data at $T = 0$, we assume that the rock contains water with no particles:

$$\sigma(X, 0) = 0 \qquad \text{and} \qquad c(X, 0) = 0. \tag{2.7}$$

From equations (2.5) and (2.6), we obtain the following ordinary differential equation along the line $X = 0$:

$$\frac{\partial \sigma(0, T)}{\partial T} = \lambda(\sigma(0, T))c_i(T) \qquad \text{and} \qquad \sigma(0, 0) = 0. \tag{2.8}$$

Integrating equation (2.8) provides $\sigma(0, T)$, which is always positive and increasing.

Remark 2.1. The system (2.4)–(2.5) can be rewritten as

$$\frac{\partial}{\partial T}\begin{pmatrix} c \\ \sigma \end{pmatrix} + \begin{pmatrix} 1 & 0 \\ 0 & 0 \end{pmatrix} \frac{\partial}{\partial X}\begin{pmatrix} c \\ \sigma \end{pmatrix} = \begin{pmatrix} -\lambda(\sigma) & 0 \\ \lambda(\sigma) & 0 \end{pmatrix}\begin{pmatrix} c \\ \sigma \end{pmatrix}, \tag{2.9}$$

which is a quasi-linear hyperbolic system. This system has two characteristic directions (see figure 1) $(\mathrm{d}X, \mathrm{d}T)^T = (1, 1)^T$ and $(\mathrm{d}X, \mathrm{d}T)^T = (0, 1)^T$, with respective speeds 1 and 0.

The notation $\frac{\mathrm{d}}{\mathrm{d}X}$ will be used to indicate differentiation along characteristic lines of speed 1, i.e., $\frac{\mathrm{d}}{\mathrm{d}X} = \frac{\partial}{\partial T} + \frac{\partial}{\partial X}$. Using this notation, the first expression in equation (2.9) becomes $\frac{\mathrm{d}c}{\mathrm{d}X} = -\Lambda$. Thus, c decreases along these characteristic lines.

According to the theory of systems of hyperbolic equations, discontinuities in the solution may occur along the characteristic line $T = X$.

2.2. Solution of the direct problem

We start with the following assumptions:

Assumption 2.2. *We assume that the experimental injected concentration c_i is a positive continuously differentiable function for $T \geqslant 0$, i.e., $c_i(T)$ is C^1.*

Assumption 2.3. *The filtration function $\lambda(\sigma)$ is a positive C^1 function of σ in $0 \leqslant \sigma < 1$.*

This assumption is somewhat stringent in practical applications because $\lambda(\sigma)$ may vanish for colloidal suspensions. From physical properties of the filtration phenomena, we consider that if $\lambda(\sigma)$ vanishes at some point $\sigma^0 \leqslant 1$, then $\lambda(\sigma) = 0$ for all σ in $[\sigma^0, 1]$. Equation (2.5) says σ is monotone increasing in time, so if it reaches σ^0 at $X = 0, T = T^0$, it becomes constant along the characteristic line $T - X = T^0$. Then, it follows from equation (2.9) that c becomes invariant along $T - X = T^0$ as well and c_e becomes constant if c_i is constant. We do not consider this possibility: assumption 2.3 restricts us to the case where c_e is monotone increasing.

From assumption 2.3, we can define the first integral Ψ of $1/\lambda$ and the quantity m as follows:

$$\Psi(\sigma) = \int_0^\sigma \frac{\mathrm{d}\eta}{\lambda(\eta)}, \qquad m = \int_0^1 \frac{\mathrm{d}\eta}{\lambda(\eta)}. \tag{2.10}$$

Note that $\Psi(0) = 0$. Depending on the behaviour of $\lambda(\sigma)$ near 1, the range of $\Psi : [0, 1) \to [0, m)$ is either a finite or infinite interval.

Theorem 2.4. *There exists a unique, well-posed weak solution in the infinite rectangle for the system (2.4)–(2.5) with initial data (2.7) and C^1 boundary data c_i. This solution vanishes in the triangle with vertices $(0, 0), (0, 1), (1, 1)$ in figure 1; it is C^1 in the trapezoid above the triangle, where it is given by the unique family of solutions of the ODEs (2.8), (2.16).*

Solution in the triangle. We consider the system (2.9) in the triangle $\{(X, T) : 0 \leqslant T \leqslant X \leqslant 1\}$ with initial data (2.7). It follows from the method of characteristics described in section 5, chapter 2 of [10] and section 2, chapter 5 of [6] that the only solution in the triangle vanishes identically. This is illustrated by the two characteristic lines reaching the point (X, T) in the triangle shown in figure 1: since σ and c vanish at the feet of characteristics, they vanish at (X, T).

Uniqueness of solution near the diagonal. Let us consider bounded weak solutions of (2.4)–(2.5) defined near the line $X = T$ (see figure 1), in the sense of [10]. Integrating (2.5) along segments with fixed X for $0 < X \leqslant 1$ from $T - \epsilon$ to $T + \epsilon$, where ϵ is positive and small, we see that

$$0 = \lim_{\epsilon \to 0^+} \{\sigma(X, T + \epsilon) - \sigma(X, T - \epsilon)\} = \lim_{\epsilon \to 0^+} \sigma(X, T + \epsilon) - 0. \tag{2.11}$$

This equation says that σ vanishes along the diagonal and it is continuous there. Performing the same integration on (2.4) yields no new information, i.e., $c(X, T)$ may be nonzero on

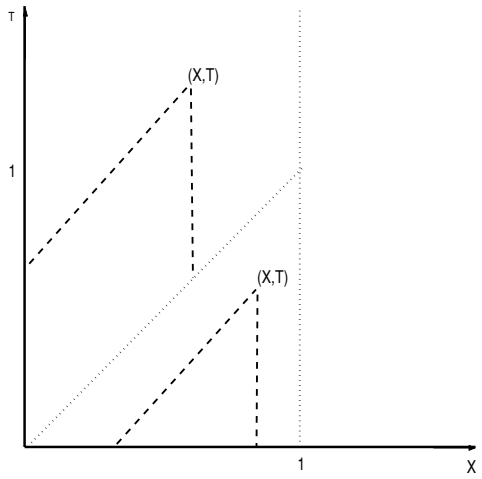

Figure 1. Characteristic lines: triangle (lower) and trapezoid (upper).

$T = X$, just above the trapezoid lower edge from $(0, 0)$ to $(1, 1)$; in other words, there is a discontinuity in c along $T = X$.

Proof of uniqueness of solution in the trapezoid. We will focus our attention on the trapezoid $\{(X, T) : 0 \leqslant X \leqslant 1, T \geqslant X \geqslant 0\}$, see figure 1. Differentiating equation (2.10) and using equation (2.5), we obtain

$$\frac{\partial \Psi(\sigma)}{\partial T} = c \qquad \text{for} \quad \sigma \in [0, 1). \tag{2.12}$$

Since Ψ is C^2, the derivatives of (2.12) are

$$\frac{\partial c}{\partial T} = \frac{\partial^2 \Psi(\sigma)}{\partial T^2} \qquad \text{and} \qquad \frac{\partial c}{\partial X} = \frac{\partial^2 \Psi(\sigma)}{\partial T \partial X}. \tag{2.13}$$

Substituting the expressions (2.12) and (2.13) into (2.4), we have

$$\frac{\partial^2 \Psi(\sigma)}{\partial T^2} + \frac{\partial^2 \Psi(\sigma)}{\partial T \partial X} = -\frac{\partial \sigma}{\partial T} \qquad \text{or} \qquad -\frac{\partial}{\partial T}\left(\frac{\mathrm{d}\Psi(\sigma)}{\mathrm{d}X}\right) = -\frac{\partial \sigma}{\partial T}, \tag{2.14}$$

which is well defined for $X \neq T$. In (2.14*b*), $\frac{\mathrm{d}}{\mathrm{d}X}$ is again the differentiation along characteristic lines $T - X =$ constant, i.e. $\frac{\mathrm{d}}{\mathrm{d}X} = \frac{\partial}{\partial X} + \frac{\partial}{\partial T}$, see figure 1.

Throughout this paper, we will use this convention to refer to one of multiple similar equations introduced in a single line, as we have just done with equations (2.14*a*) and (2.14*b*), which are the left and right equations, respectively.

Now, we consider (2.14) in the infinite trapezoid $\{(X, T) : 0 \leqslant X \leqslant 1, T \geqslant X \geqslant 0\}$. Integrating (2.14*b*) in T along a vertical line from the point (X, X) on the lower edge of the trapezoid to a fixed (X, T), we obtain

$$\left.\frac{\mathrm{d}\Psi(\sigma)}{\mathrm{d}X}\right|_{(X,T)} - \left.\frac{\mathrm{d}\Psi(\sigma)}{\mathrm{d}X}\right|_{(X,X)} = \sigma|_{(X,T)} - \sigma|_{(X,X)}. \tag{2.15}$$

Equation (2.10) implies that $\sigma|_{T=X} = 0$, so $\Psi(\sigma)|_{T=X} = \Psi(0)$ and $\frac{\mathrm{d}}{\mathrm{d}X}\Psi(\sigma)|_{T=X} = 0$; using these expressions and (2.10) in (2.15) we obtain (2.16*a*); then, using equations (2.4) and (2.5), we obtain (2.16*b*)

$$\frac{\mathrm{d}\sigma}{\mathrm{d}X} = -\lambda(\sigma)\sigma \qquad \text{and} \qquad \frac{\mathrm{d}c}{\mathrm{d}X} = -\lambda(\sigma)c. \tag{2.16}$$

In summary, we have proved under assumptions 2.2 and 2.3 that if (2.4)–(2.5) has a C^1 solution in the trapezoid satisfying equations (2.7) and (2.8), then this solution must satisfy (2.16) in the trapezoid. □

Proof of existence of solution in the trapezoid. Let us focus on the infinite trapezoid $\{(X, T) : 0 \leqslant X \leqslant 1, T \geqslant X \geqslant 0\}$. Consider the unique C^1 solution $\sigma(X, T)$, $c(X, T)$ of (2.8) and (2.16) in the trapezoid. Note that (2.15), (2.14), (2.13) and (2.12) hold, therefore (2.4)–(2.5) hold and this is the only solution of system (2.4)–(2.7) in the trapezoid.

In summary, under assumptions 2.2 and 2.3, the system (2.4)–(2.7) has a unique solution on the infinite rectangle. This solution has a jump in c along the front $X = T$. This is the unique global weak solution of (2.4)–(2.5) under proper initial and boundary conditions and assumption 2.3. This completes the proof of theorem 2.4. □

Remark 2.5. The system of equations (2.8), (2.16) is convenient for the theory as well as for using standard ODE procedures to solve numerically the PDE. This system is solved as follows. First, we solve the ODE (2.8) to find $\sigma(0, T)$. Then we solve along characteristic lines the ODE (2.16*a*) with data $\sigma(0, T)$ to find σ on the trapezoid. If we want to find c also, we solve along characteristic lines the system (2.16) with data $\sigma(0, T)$ and $c_i(T)$.

Remark 2.6. If we take the experimental data function $c_i(T)$ to be C^2 instead of C^1, then the solution σ, c of the system (2.4)–(2.7) is C^2 in the trapezoid. In particular, the predicted effluent concentration $c(1, T)$ is a C^2 function.

2.3. The invariant along characteristics

Except at initial times, it turns out that c is much smaller than σ. Because of this fact, Herzig *et al* [8] proposed a simplified model comprising (2.5) and the following modified version of (2.4), where $\partial c/\partial T$ in (2.4) was neglected relative to $\partial\sigma/\partial T$:

$$\frac{\partial\sigma}{\partial T} + \frac{\partial c}{\partial X} = 0. \tag{2.17}$$

For the model (2.5) and (2.17), under the assumption in equation (2.7*a*) Herzig *et al* in [8] proved the following relationship between the deposited and suspended particle concentrations along characteristic lines:

$$\frac{\sigma(X, T)}{c(X, T)} = \frac{\sigma(0, T)}{c(0, T)},$$

which is valid for $T > 0, 0 \leqslant X \leqslant 1$. However, an analogous relationship was stated in [4] for the full model (2.4)–(2.5) based on an incomplete derivation. Because the relationship in [4] is the basis of the method for determining $\lambda(\sigma)$, we provide a proof for it.

Lemma 2.7. *Consider the solution of (2.4)–(2.7) under assumptions 2.2 and 2.3. Then, σ/c is constant along characteristic lines with slope 1 emanating from the positive vertical axis.*

From equations (2.16*a*) and (2.16*b*), we obtain along characteristic lines

$$\frac{\mathrm{d}\sigma}{\mathrm{d}c} = \frac{\sigma}{c}.$$

Integrating this equation along characteristic lines with slope 1, we obtain that σ/c is invariant along such lines; hence, we have

$$\frac{\sigma(X, T)}{c(X, T)} = \frac{\sigma(0, T - X)}{c(0, T - X)}. \tag{2.18}$$

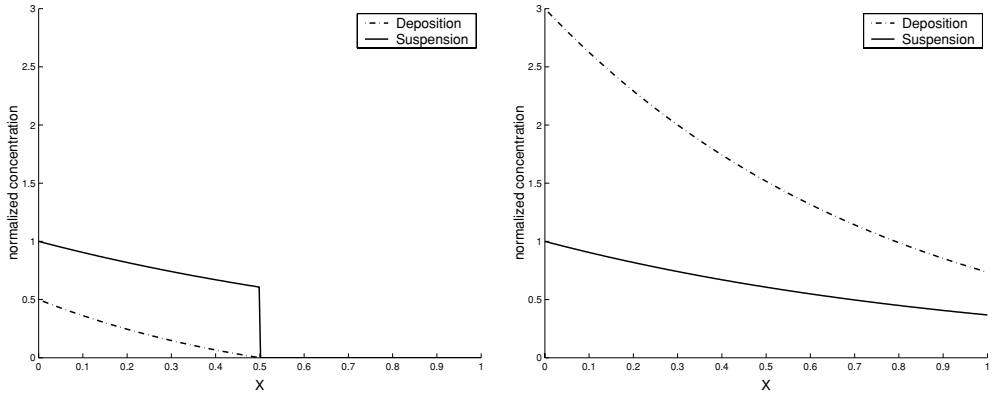

(a) $T = 0.5\,\mathrm{PVI}$ (b) $T = 3\,\mathrm{PVI}$

Figure 2. Typical normalized suspended and deposited particle concentrations before and after breakthrough: note the discontinuity at $T = X$ in (a).

Remark 2.8. Since along the front trajectory $X = T$ the deposited concentration is zero, from (2.16*b*), we obtain the following ordinary differential equation for $c(X, X)$ along this line in the trapezoid:

$$\frac{\mathrm{d}c(X, X)}{\mathrm{d}X} = -\lambda(0)c(X, X). \tag{2.19}$$

Integrating (2.19) and using (2.6) at $T = 0$, we obtain

$$c(X, X) = c_i(0)\exp(-\lambda(0)X). \tag{2.20}$$

Since $c_i(0) > 0$, from (2.20) we obtain that $c(X, X)$ is positive for $X > 0$ in the trapezoid and 0 below; so there is indeed a discontinuity along the characteristic $X = T$, as shown in figure 2(a).

3. The recovery method

Here, we describe the recovery method for obtaining the filtration function in (2.9) from the injected and effluent concentration of particles. See also [1, 2, 4, 11, 12]. An inverse problem for a system similar to (2.9) was studied in [5].

3.1. Derivation of the functional equation

Here, we generalize [2, 4], where only the case of constant injected concentration $c_i(T) = c_{i0}$ was considered. It is useful to introduce the notation

$$c_i(z) > c_e(z) > 0, \qquad \sigma_i(z) = \sigma(0, z), \qquad \sigma_e(z) = \sigma(1, z + 1), \tag{3.1}$$

where $z \geqslant 0$ indicates dimensionless time, but shifted by 1 in the function σ_e and the data c_e. The subscript e indicates 'effluent' or $X = 1$, in accordance with the subscript i indicating 'injected' or $X = 0$.

Assumption 3.1. *The experimental data c_i, c_e are C^2 functions for $0 \leqslant z < \infty$, satisfying $c_e(z) < c_i(z)$.*

The motivation for this assumption is that Λ should be positive, see remark 2.1. We need the following:

Definition 3.2. *The data c_i, c_e satisfying assumption 3.1 are said to conform to the model if there is a $\lambda(\sigma) > 0$ for which the solution of (2.4)–(2.7) gives rise to a function $c(X, T)$ such that $c(1, z + 1) = c_e(z)$ for $z \geqslant 0$.*

We will also utilize the C^3 functions on $0 \leqslant z < \infty$

$$\tau = C_i(z) \equiv \int_0^z c_i(s)\,\mathrm{d}s, \qquad C_e(z) \equiv \int_0^z c_e(s)\,\mathrm{d}s. \tag{3.2}$$

From (3.1*a*), it follows that C_i in (3.2*a*) is monotone increasing and $C_i(0) = 0$. Thus, from the implicit function theorem, the inverse function $C_i^{(-1)}(\tau)$ of C_i in (3.2*a*) exists and it is C^3. Moreover, this function is monotone increasing. We have

$$z = C_i^{(-1)}(\tau) \qquad \text{or} \qquad \frac{\mathrm{d}z}{\mathrm{d}\tau} = \frac{1}{c_i(z)} \qquad \text{with} \quad z(0) = 0.$$

Let us consider data that conform to the model. Relationships between the deposited and suspended particle concentrations at the inlet and outlet points $X = 0$ and $X = 1$ can be obtained as follows. We integrate equation (2.12) in z, use (3.2) and $\sigma_i(0) = \sigma(0, 0) = 0$, $\sigma_e(0) = \sigma(1, 1) = 0$, i.e.,

$$\Psi(\sigma_i(z)) = C_i(z), \qquad \Psi(\sigma_e(z)) = C_e(z). \tag{3.3}$$

We note that the existence of a Ψ satisfying (3.1) and with positive first Ψ' is equivalent to data conformance. Because of assumption 2.3, the definition (2.10) and $\Psi'(\sigma) = 1/\lambda(\sigma) > 0$, there exists the function $g : [0, m) \to [0, 1)$, with $g(0) = 0$:

$$\sigma = g(\psi), \qquad \text{inverse of the function} \quad \psi = \Psi(\sigma). \tag{3.4}$$

To determine Ψ, we proceed as follows. From (3.3) and (3.4), we obtain

$$\sigma_i(z) = g(C_i(z)), \qquad \sigma_e(z) = g(C_e(z)) \qquad \text{for} \quad z \geqslant 0. \tag{3.5}$$

Replacing X by 1 and T by $T + 1$ in (2.18) and using (3.1) with $z = T$, we obtain

$$\frac{\sigma(1, T + 1)}{c(1, T + 1)} = \frac{\sigma(0, T)}{c(0, T)} \qquad \text{or} \qquad \frac{\sigma_e(z)}{c_e(z)} = \frac{\sigma_i(z)}{c_i(z)}. \tag{3.6}$$

Substituting the expressions (3.5) into equation (3.6*b*), we obtain the following functional equation for the function $\sigma = g(\psi)$:

$$g(C_e(z)) = \frac{c_e(z)}{c_i(z)} g(C_i(z)) \qquad \text{or} \qquad g(C_e(z)) = \frac{C_e'(z)}{C_i'(z)} g(C_i(z)) \qquad \text{for} \quad z \geqslant 0. \tag{3.7}$$

Finally, using the definition of τ in (3.2) and denoting

$$D(\tau) \equiv C_e\big(C_i^{(-1)}(\tau)\big) \qquad \text{and} \qquad \theta(\tau) \equiv \frac{c_e\big(C_i^{(-1)}(\tau)\big)}{c_i\big(C_i^{(-1)}(\tau)\big)}, \tag{3.8}$$

equation (3.7) can be rewritten as

$$g(D(\tau)) = \theta(\tau) g(\tau) \qquad \text{for} \quad \tau \geqslant 0. \tag{3.9}$$

Here D and θ are known, so this is a functional equation for g that needs to be solved.

Remark 3.3. Note that $D \in C^2(0, r]$ and $D(0) = 0$. It follows from equations (3.2) and (3.8) that

$$\frac{\mathrm{d}D(\tau)}{\mathrm{d}\tau} = \frac{c_e(z)}{c_i(z)} \qquad \text{for} \quad \tau = C_i(z). \tag{3.10}$$

Integrating this along a characteristic from $(X, T) = (0, z)$ to $(1, z + 1)$, we see from (2.16*b*) that

$$c_e(z)/c_i(z) = \exp\left(-\int_0^1 \lambda(\sigma(z, z+s))\,\mathrm{d}s\right). \tag{3.11}$$

Let us consider data satisfying assumption 3.1. From equations (3.8*b*) and (3.11), it follows that $\theta(\tau) < 1$. We also conclude that $\frac{\mathrm{d}}{\mathrm{d}T} D(T) < 1$, since the average value of $\lambda(\sigma)$ is positive along the characteristic line, so $D : [0, r] \to [0, r)$ satisfies $D(\tau) < \tau$.

3.2. Derivation of an iterative formula for the functional equation

We present an algorithm or formula for finding g in (3.9): to compute $g(\tau_0)$ for any $0 < \tau_0 < r$, we define the two infinite sequences

$$\begin{aligned} &\tau_1 = D(\tau_0), \qquad &&\tau_2 = D(\tau_1), \qquad \ldots \qquad &&\tau_n = D(\tau_{n-1}), \\ &q_1 = \theta(\tau_0), \qquad &&q_2 = \theta(\tau_1)q_1, \qquad \ldots \qquad &&q_n = \theta(\tau_{n-1})q_{n-1}, \end{aligned}$$

or

$$\tau_n = D^n(\tau_0), \qquad q_n = \prod_{k=0}^{n-1} \theta(\tau_k).$$

For conforming data, let D be the function in remark 3.3. Given any point $\tau_0 \in (0, r]$, the non-negative sequence in $[0, r]$ given by $\tau_{n+1} = D(\tau_n), n \geqslant 0$, is monotone decreasing and converges to 0 (see [1] or [11] for a proof). Note that $\tau_1 = D(\tau_0)$ is continuous in τ_0 and so is $\tau_n = D^n(\tau_0)$. Similarly, since θ is continuous, q_n is a continuous function of τ_0; also, because $\theta < 1, q_n$ is a monotone decreasing sequence. Finally, it is proven in [11] that $\lim_{n\to\infty} q_n(\tau_0) = 0$ uniformly for $\tau_0 \in [0, r)$.

From the functional equation (3.9), it follows that

$$g(\tau_k) = g(D(\tau_{k-1})) = \theta(\tau_{k-1})g(\tau_{k-1}),$$

so by repeated use of the above formula for $k = n, n - 1, \ldots, 1$, we obtain

$$g(\tau_n) = g(\tau_0) \prod_{k=0}^{n-1} \theta(\tau_k). \tag{3.12}$$

On the other hand, using the definition of derivative and $g(0) = 0$, we obtain

$$g'(0) = \lim_{n\to\infty} \frac{g(\tau_n) - g(0)}{\tau_n - 0} = \lim_{n\to\infty} \frac{g(\tau_n)}{\tau_n}\cdot \tag{3.13}$$

Substituting (3.12) into (3.13), we see that

$$g'(0) = g(\tau_0) \lim_{n\to\infty} \frac{\prod_{k=0}^{n-1} \theta(\tau_k)}{\tau_n} \qquad \text{or} \qquad g(\tau_0) = g'(0) \lim_{n\to\infty} \frac{\tau_n}{q_n}\cdot \tag{3.14}$$

We have obtained the solution for the functional equation (3.9) for any $\tau_0 > 0$.

Formula (3.14*b*) can be rewritten as an infinite product, which is very useful for analysis and numerical calculations. Let us define

$$R_n = \frac{\tau_n}{\prod_{k=0}^{n-1} \theta(\tau_k)}, \qquad \rho_n = \frac{D(\tau_n)}{\theta(\tau_n)\tau_n}\cdot \tag{3.15}$$

Then,

$$R_n = \frac{D(\tau_{n-1})\tau_{n-1}}{\theta(\tau_{n-1})\tau_{n-1}\prod_{k=0}^{n-2} \theta(\tau_k)} = \frac{D(\tau_{n-1})}{\theta(\tau_{n-1})\tau_{n-1}} R_{n-1} = \rho_{n-1}R_{n-1}, \tag{3.16}$$

so that

$$g(\tau_0) = g'(0)\prod_{n=0}^{\infty}\frac{D(\tau_n)}{\theta(\tau_n)\tau_n} \qquad \text{or} \qquad g(\tau_0) = g'(0)\prod_{n=0}^{\infty}\rho_n. \tag{3.17}$$

Equation (3.17) is the basis of the algorithm for solving the functional equation. Of course, we have not proven the convergence of (3.17): this point is addressed in the next section.

Once (3.17) is solved, from the definitions of g in (3.4) and Ψ in (2.10), we obtain

$$\lambda(\sigma) = g'(\sigma). \tag{3.18}$$

Thus, once the function $\sigma = g(\Psi)$ has been found by means of equation (3.9), we determine the filtration function $\lambda(\sigma)$ by differentiating g.

Remark 3.4. Note from (3.18) that $g'(0) = \lambda(0)$. This value is determined from (2.20) as follows:

$$g'(0) = \lambda(0) = -\log(c_e(0)/c_i(0)). \tag{3.19}$$

The positivity requirement in assumption 2.2 is imposed so that (3.19) can be used to determine $\lambda(0)$.

3.3. Existence and uniqueness of the solution of the functional equation

In this section, we prove that the functional equation (3.9) is solved by equation (3.17), using the results for the existence and uniqueness of the solution of (3.9) given in [12]. We assume that the data $c_i(T)$, $c_e(T)$ satisfy assumption 3.1.

In practice, the values of the injected and effluent particle concentration are measured up to the final time T_f. So, we solve equation (3.9) for τ in $[0, r]$, where $r = C_i(T_f)$. Let us consider the Banach space

$$G_2^0 = \{g \in C^2[0, r], \text{ such that } g(0) = 0\}$$

with norm

$$\|g\| = \sup_{x\in[0,r]}\{|g(x)|\} + \sup_{x\in[0,r]}\{|g'(x)|\} + \sup_{x\in[0,r]}\{|g''(x)|\}.$$

Theorem 3.5. *Let $D : [0, r] \to [0, r)$ be a C^2 monotone increasing function, such that $D(0) = 0$ and $D(\tau) < \tau$ in $(0, r]$. Let $\theta : [0, r] \to (0, 1)$ be a C^2 function, satisfying $0 < \theta(\tau) < 1$ and $[D'(0)]^2/\theta(0) < 1$. Furthermore, consider the functional equation (3.9) on G_2^0, i.e.,*

$$g(D(\tau)) = \theta(\tau)g(\tau) \qquad \textit{for} \quad \tau \in (0, r).$$

Then the functional equation (3.9) has a solution $g \in G_2^0$, which is uniquely defined by the value of $g'(0)$.

Proof. For data satisfying assumption 3.1, remark 3.3 shows that $0 < \theta(\tau) < 1$ for $\tau \geqslant 0$. Moreover, for conforming data, one verifies using (3.8) that $D'(0) = \theta(0)$, so the inequality $[D'(0)]^2/\theta(0) = \theta(0) < 1$ is satisfied and $D(\tau) < \tau$ for $\tau > 0$. Finally, $D(\tau)$ and $\theta(\tau)$ are C^2 functions because the functions c_i and c_e are C^2.

The existence of a unique C^2 solution g of the functional equation (3.9) is guaranteed by theorem 3.4.2 in [12]. The iterative formula presented in the previous section for the solution of (3.9) is theorem 5.8 in [11]. □

Remark 3.6. If the data do not conform to the model but the hypotheses of theorem 3.5 hold, then the functional equation still has a unique solution g. However, there is no guarantee that $g' > 0$.

Remark 3.7. If the solution g of the functional equation (3.9) has positive derivative, which is not true for all input data, we can solve the direct problem (2.4)–(2.7) using the filtration function $\lambda(\sigma)$ determined by (3.18) and find $c(1, T)$. One can verify, using the method described here and theorem 3.5, that the corresponding effluent concentration function $c(1, T)$ coincides with the input data $c_e(T)$ used in the recovery procedure.

We have proved the following:

Theorem 3.8. *Consider the data $c_i(T)$, $c_e(T)$ satisfying assumption 3.1, such that D and θ satisfy the hypotheses of theorem 3.5. Then there exists a unique $g(\tau) \in C^1$. If $g' > 0$, then $\lambda(\sigma)$ is uniquely defined and the problem (2.4)–(2.7) has a unique solution, which satisfies $c(1, T) = c_e(T)$, i.e., those data conform to the model.*

Remark 3.9. Conforming data certainly satisfy the hypotheses of theorem 3.8, with $g' > 0$.

Remark 3.10. More generally, it is possible to prove that given C^m functions $c_i(T)$, $c_e(T)$, the filtration function $\lambda(\sigma)$ is C^{m-1}.

Remark 3.11. For constant injected concentration $c_i(z) = c_{i0}$, (3.9) reduces to Julia's equation, which is studied in [12]:

$$g(D(\tau)) = D'(\tau)g(\tau) \qquad \text{for} \quad \tau \geqslant 0. \tag{3.20}$$

The recovery method outlined in [4] is based on the functional equation (3.20) and a formula for its solution is obtained by an analogous iterative procedure. Here, the formula for the solution $g(\tau)$ of (3.9) was obtained for non-constant injected concentration $c_i(T)$. The derivation of the general case and Julia's formula are the same, whereas the notation in Julia's case is less cumbersome; in fact, for Julia's equation the formula (3.17) reduces to

$$g(\tau_0) = g'(0) \prod_{n=0}^{\infty} \frac{D(\tau_n)}{D'(\tau_n)\tau_n}, \qquad \text{with} \quad D(\tau) = C_e(\tau/c_{i0}). \tag{3.21}$$

Remark 3.12. If $\lambda(\sigma) = 0$ in $[\sigma^0, 1]$ (see section 2.2) and $\lambda(\sigma) > 0$ in $[0, \sigma^0)$, the procedure described above can still be used prior to the time T^0 when $\sigma(0, T^0)$ reaches σ^0. It breaks down completely if one tries to apply it to data for $T \geqslant T^0$.

4. Regularity

In summary, the method for obtaining the filtration function in section 3 consists of the following sequence of calculations:

$$\{c_i, c_e\} \to \{C_i, C_e\} \to \{D, \theta\} \to g \to \lambda = g',$$

where '$\to$' represents a procedure to obtain output functions from the previous data. To obtain numerical methods for calculating a regular approximate solution of the filtration function, we must study the well-posedness of equations (3.2), (2.10) and (3.9).

Clearly, the functions C_i and C_e depend continuously on c_i and c_e, respectively. The functions D and θ depend continuously on c_i, c_e as well. In [12], it was proved that the solution of the functional equation (3.9) depends continuously on the functions $D(\tau)$ and

$\theta(\tau)$, so the solution g depends continuously on the functions c_i and c_e. If c_i and c_e are C^m, then $g \in C^m$. Continuous dependence of m derivatives of g is established under changes in c_i and c_e measured in terms of the mth derivative. This is a consequence of many results given in chapter 3 of [12]. A proof of regularity is found in the appendix.

The regularity of the numerical solution obtained by the recovery method requires that the numerical differentiation of the solution g of (3.9) is performed in a stable way. We have tested both cubic and quintic smoothing splines for numerical differentiation, but the solutions obtained were not significantly different to justify the higher order approximation. Also, we can expect that serious numerical instabilities arise when the filtration function values are very small, as they appear in the denominator of (2.10) that defines Ψ.

5. Numerical results

In this section, the implementation of the numerical method for solving the functional equation is described, along with the experiments we performed over real measurement data, their results and brief discussion.

5.1. Implementation

We have implemented the product form presented in (3.21) (Julia's equation), assuming that $c_i(T)$ is a constant c_{i0}. The algorithm takes this constant and a time series $(T, c_e(T))$ as input.

We performed synthetic experiments by prescribing smooth monotone decreasing $\lambda(\sigma)$, with c_i constant and calculating $c_e(T)$. When a fine temporal grid for $c_e(T)$ was used, the recovery procedure for $\lambda(\sigma)$ worked surprisingly well, yielding a recovered $\lambda(\sigma)$ that was indistinguishable from the prescribed one. Short from the intrinsic truncation errors, the direct and inverse problems yielded perfect matches in these synthetic experiments. We now describe and present the results for experimental data obtained from [13].

Experimental data were filtered so that only the pairs with $T \geqslant 1$ for which $c_e(T) > 0$ are used. Ideally, the time value T_0 of the first of these pairs is 1, but not in practice: in the four real cases we studied, it was in the range [4.26, 7.75]. To provide for the missing datum $c_e(1)$ and also to obtain a dense data set from the sparse points available, we have added arbitrarily the point $(T = 0,\ c_e(0) = 0)$ to the data series and then we used cubic spline interpolation to obtain a smooth, dense set which includes the point $(1,\ c_e(1))$. As we pointed out in section 4, the use of higher order (i.e., quintic) smoothing splines did not significantly improve the solutions obtained.

The time series are not necessarily evenly spaced. Over this time grid we compute the auxiliary quantity $D(\tau)$, using standard trapezoidal integration. Next we compute the cubic spline used to evaluate the function $D(\tau)$, stored as a discrete series, and its derivative. Since $D(\tau)$ is the integral of $c_e(T)$, we know its first derivative at the end points, and use it when computing the spline coefficients.

We now proceed to the computation of $g(\tau)$ as in (3.21). We create an evenly spaced mesh for Ψ in (2.10) covering the interval $[0, T_f]$, the whole span for which data are available. Over this mesh, we compute the values of g iteratively as a truncated infinite product. The criterion for truncation is the quotient τ_n/q_n dropping to zero or its relative difference to τ_{n-1}/q_{n-1} becoming less than 10^{-4}. These values were determined through experimentation. We decided to use an evenly spaced mesh for simplicity, as the computation of any $g(\tau_0)$ requires the computation of g for many other values in the interval $[0, \tau_0]$.

If the model (2.4)–(2.7) were a proper description of reality, $g(\tau)$ would be non-decreasing and $g'(\tau) = \lambda(\sigma)$ would be non-negative; but using experimental data yielded

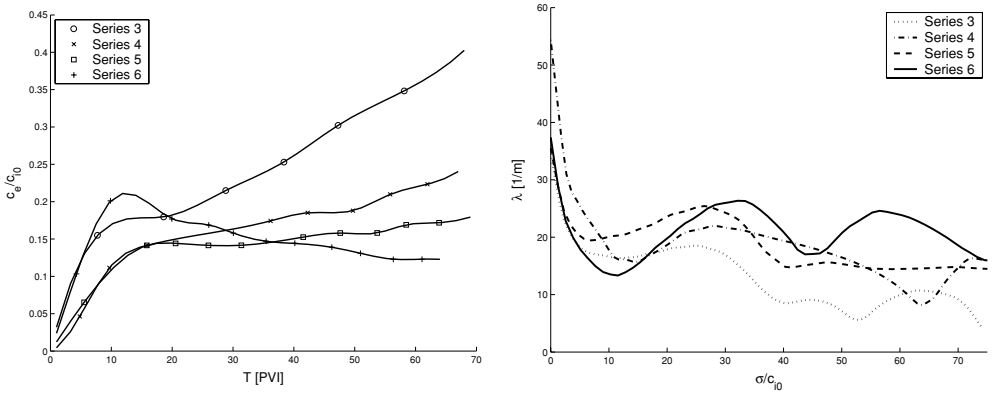

(a) Effluent profiles (b) Filtration functions

Figure 3. The markers in (a) show the data series for which we solved the inverse problem. The solid curves are the effluent concentrations calculated on the basis of the recovered filtration functions (b).

non-monotonical $g(\tau)$ profiles. We analysed six data sets from [13], and for four of those we obtained good results working around the lack of monotonicity by removing the decreasing intervals of $g(\tau)$, forcing it to stay constant at the maximum at the left of each such interval. Finally, we use $g(\tau)$ to evaluate $\lambda(\sigma)$ as given in (3.18).

Figure 3 shows our primary results: in figure 3(a), we show as markers the original data points of the series 3 through 6 we obtained from [13], and the preprocessed data are shown as solid curves over the markers. For each of these data series, the corresponding $\lambda(\sigma)$ was recovered; these are shown in figure 3(b). They are all different, as the physical situation was different in each experimental series in [13]. Finally, the effluent profiles found by solving the direct problems using each recovered $\lambda(\sigma)$ are shown as solid curves in figure 3(a) and they coincide visually with the input data. The oscillations in the filtration functions are due to insufficient smoothness of the data sets. Smoother data would yield smoother filtration profiles.

5.2. The effect of extrapolating for missing data

Experimental data for the breakthrough concentration $c_e(1)$ are usually unavailable. This difficulty arises from the small value of σ at breakthrough and from diffusive effects. The value of $c_e(1)$ is a key scaling factor for the whole procedure, so the influence of this value over the procedure was tested in the second experiment. We repeated the previous runs using the same data processing as in section 5.1, but now setting $c_e(1) = c_e(T_0)$, where $T_0 > 1$ is the actual time value of the first data point available where $c_e > 0$. Except near $T = 1$, the resulting effluent concentration data series are identical to those used previously. As can be seen in figure 4, the filtration functions recovered from these series are very similar to the previous ones, except for very low σ values, i.e., changes in $c_e(1)$ affected mostly values of λ in the neighbourhood of $\sigma = 0$, as expected. For higher σ values, there is little change in the effluent profiles produced using the filtration functions recovered through the functional equation, despite the unavailability of the $c_e(1)$ datum. One can set the value of $c_e(1)$ quite arbitrarily without affecting the shape of the filtration function for higher σ values.

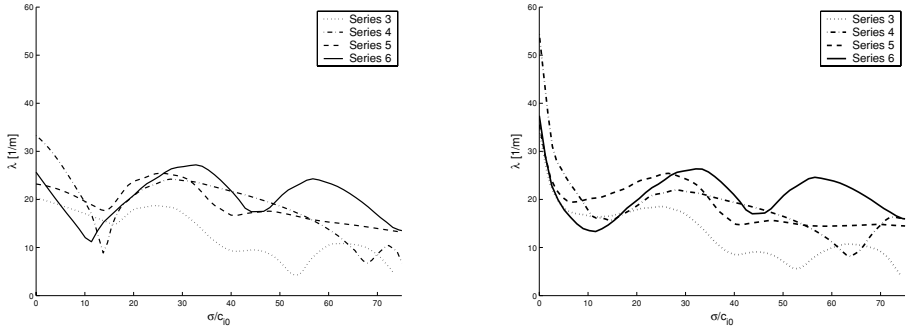

(a) Filtration functions for data with imposed $c_e(1)$ (b) Filtration functions from previous experiment

Figure 4. (a) The filtration coefficients obtained from the series where the value of $c_e(1)$ was imposed. (b) Same as figure 3(b). Comparing both figures, note the difference for low σ and the similarity of the profiles as σ increases.

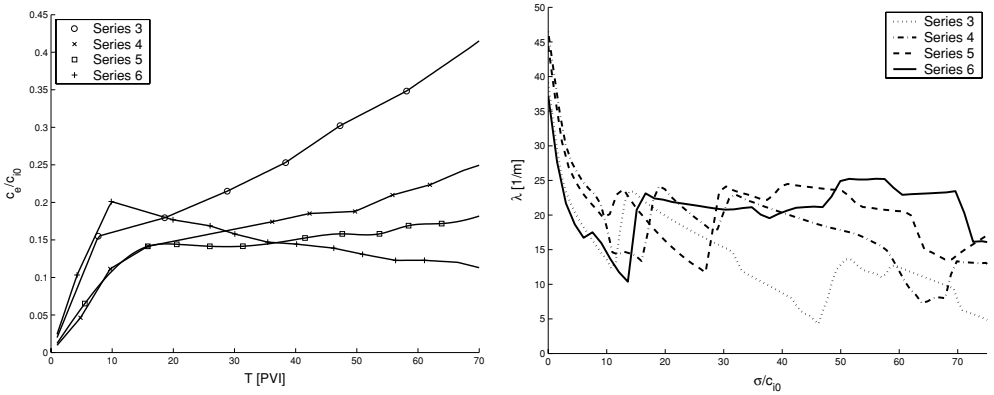

(a) Effluent profiles (b) Filtration functions

Figure 5. Third experiment. Same as in figure 3, but using linear interpolation when preprocessing the effluent profile data.

5.3. The impact of data smoothing

In our next experiment, we used a fine mesh and linear interpolation before smoothing the data with the cubic splines, so as to preserve their sharp edges. The results are analogous to those of the first experiment. Figure 5(a) shows the input data, which are the same data from section 5.1, but with different preprocessing—compare with figure 3(a). Figure 5(b) shows the filtration functions recovered from these data. Once again, solving the direct problems with the recovered filtrations reproduces the input data with great accuracy, so they coincide visually with the input data shown in figure 5(a). Note the filtration functions show the same oscillating nature, however more edgy. The oscillations are therefore due to higher values of the low-order derivatives of the curves implied by the data series.

5.4. The effect of data preprocessing

As long as g' is sufficiently positive, the solution of the direct problem using the filtration function recovered with this procedure yields the input data series exactly, accounting for all its

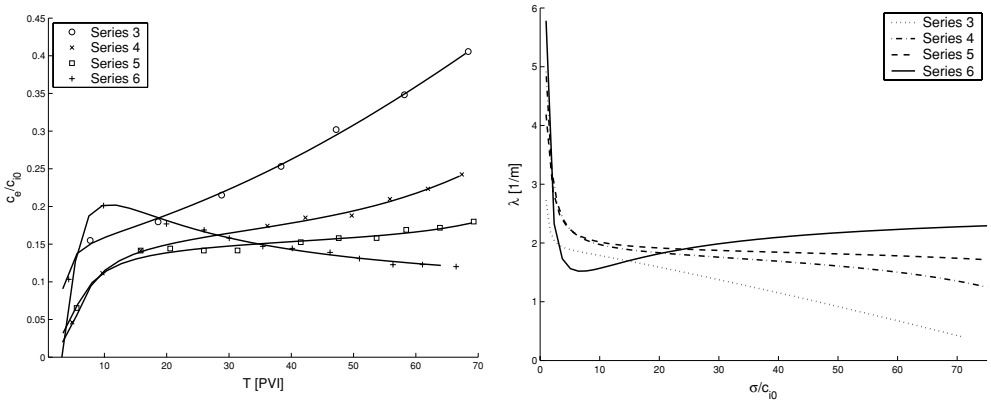

(a) Smooth profiles obtained from data

(b) Corresponding filtration functions

Figure 6. Exact recovery obtained using the functional equation over smooth approximation of the actual data.

irregularities. However, because of experimental error, it is common practice in engineering to preprocess the data and replace them with smooth curves that do not necessarily pass through the experimental points; usually some sort of least-squares approximation is used. Figure 6(a) shows smooth profiles obtained from the data points using a preprocessing method described in a forthcoming work; applying the algorithm described here to these profiles yielded the extremely smooth filtration functions shown in figure 6(b), which look much more reasonable than those in figure 4(b). We calculated the effluent concentrations using these filtrations and plotted them over the input data in figure 6(a); once again, they coincide visually.

6. Conclusion

The method described here reduces the inverse problem of recovering the empirical filtration coefficient from measurements of effluent concentration to solving a functional equation. Taking smooth experimental data functions we obtain a nice inverse problem, with a unique solution. We presented a stable numerical method which, short of numerical errors, provides perfect matching between prescribed and predicted data, both for synthetic and for conforming experimental data. As long as the effluent concentration is sufficiently smaller than the injected concentration, the method is not unduly impaired by the lack of the breakthrough data on which the calculations rely and maintains consistency with the raw data through different filtering approaches at the preprocessing stage. The quality of the recovered filtration functions depends heavily on the type of preprocessing done, and good preprocessing methods should be further investigated.

Alternatively, experimental research to determine typical forms or parametrizations for the filtration function in physical situations that conform to the model could presumably eliminate the need for preprocessing. In chapter 4 of [12], it is shown that if c_i and c_e are locally analytic, i.e., if they have convergent power series, then so is g and therefore λ. This fact provides a motivation for parametrizing analytic expressions for the filtration function and utilizing a least-squares method to obtain values of the parameters that best fit the data. If this approach turns out to yield better numerical procedures for solving the inverse problem than the one described here, the value of this work is to show that, under well-defined mathematical

assumptions, this inverse problem has a unique regular solution, hence it makes sense to look for it.

Acknowledgments

The authors are very grateful to the journal of Inverse Problems's referee, whose constructive and encouraging suggestions led to a significant improvement of this paper. The authors are grateful to Engs Alexandre G de Siqueira, Antonio Luiz Serra and Dr Eng Farid Shecaira for encouragement and support during the solution of this problem and for many useful discussions. We are grateful to Diogo Rocha Fonseca, Marcos José da Silva and Carlos Iljich Ramirez for providing digitized data. This work was supported in part by CNPq under grant 301532/2003-06; FAPERJ under grants E-26/150.408/2004 and E-26/150.163/2002.

Appendix. Stability

In order to avoid cumbersome notation, rather than studying the complete functional equation (3.9), we present here a proof for Julia's equation (3.20). First, we prove that the solution of (3.20) and its derivative belong to a certain class of uniformly bounded functions.

A.1. Regularity

Theorem A.1. *Let $D(\tau) \in [0, b]$ be a real non-negative function with continuous derivative, possessing continuous D'' derivative near 0 and satisfying*

$$\begin{aligned} &0 \leqslant D(\tau) < \tau, \qquad 0 < D'(\tau) < d < 1 \qquad \text{for} \quad 0 \leqslant \tau \leqslant b; \\ &D(0) = 0 \qquad\quad \text{and} \quad D''(0) \neq 0, \end{aligned} \tag{A.1}$$

where d is a constant.

Let $\mathcal{F}$ be the set of functions satisfying the condition (A.1) for which there exists a constant d_1 such that

$$\frac{D''(\tau) - 2D'(\tau)}{D'(0)} < d_1, \qquad \text{for all} \quad \tau \in [0, b].$$

Let us take the class of solutions $\mathcal{G}$ of the functional equation (3.9) such that $g(0) = 0$, $g'(0) \neq 0$ and $g'(0) < d_2$ uniformly. Then the solution g of the functional equation (3.9) for $D \in \mathcal{F}$ is uniformly bounded by $d_2\, \mathrm{e}^{1/(1-d)}$, and g' is uniformly bounded by $d_1 d_2\, \mathrm{e}^{1/(1-d)}$.

Proof. A necessary and sufficient condition for the existence of the infinite product in equation (3.17) is obtained by taking its logarithm; if the series of logarithms below converges, then the infinite product (3.17) exists:

$$\sum_{n=0}^{\infty} \log \rho_n = \sum_{n=0}^{\infty} \log \frac{D(\tau_n)}{D'(\tau_n)\tau_n}. \tag{A.2}$$

We recall that $\lim \tau_n = 0$, D' is uniformly continuous near 0 and $D'(0) \neq 0$ from condition (A.1); then,

$$\rho_n = \frac{D(\tau_n)}{D'(\tau_n)\tau_n} = \frac{\int_0^1 D'(\tau_n \xi)\, \mathrm{d}\xi}{D'(\tau_n)}, \qquad \text{so} \quad \lim \rho_n = \frac{\int_0^1 D'(0)\, \mathrm{d}\xi}{D'(0)} = 1.$$

We know that $\lim \tau_n = 0$ monotonically, thus there exists an N large enough so that for all $n > N$ we can use Taylor's formula in an interval $(0, \tau_n)$ where D'' exists. Since $D(0) = 0$, we obtain

$$D(\tau_n) = \tau_n D'(0) + \frac{\tau_n^2}{2} D''(\xi_n) \qquad \text{where} \quad 0 < \xi_n < \tau_n$$

and

$$D'(\tau_n) = D'(0) + \tau_n D''(\eta_n) \qquad \text{where} \quad 0 < \eta_n < \tau_n. \tag{A.3}$$

Note that to divide by $D'(\tau_n)$, we need $D'(0) \neq 0$; so, from equations (A.3)

$$\rho_n = \frac{D(\tau_n)}{D'(\tau_n)\tau_n} = \frac{(D'(0) + (\tau_n/2)D''(\xi_n))\tau_n}{(D'(0) + \tau_n D''(\eta_n))\tau_n} = \frac{1 + (\tau_n/2)(D''(\xi_n)/D'(0))}{1 + \tau_n(D''(\eta_n)/D'(0))}.$$

By further increasing N, using the continuity of D'' at zero and $D'' \neq 0$, we can ensure that $|\tau_n D''(\eta_n)|D'(0) < 1$, so that

$$\rho_n = 1 - \tau_n \frac{D''(\xi_n)/2 - D''(\eta_n)}{D'(0)} + O\big(\tau_n^2\big).$$

Using that $\log(1 + x) = x + O(x^2)$,

$$\log \rho_n = \log \frac{D(\tau_n)}{D'(\tau_n)\tau_n} \cong -\tau_n \frac{(D''(\xi_n)/2 - D''(\eta_n))}{D'(0)}.$$

Thus,

$$\frac{\log \rho_n}{\log \rho_{n-1}} = \frac{\log(D(\tau_n)/D'(\tau_n)\tau_n)}{\log(D(\tau_{n-1})/D'(\tau_{n-1})\tau_{n-1})} \cong \frac{-\tau_n(D''(\xi_n)/2 - D''(\eta_n))/D'(0)}{-\tau_{n-1}(D''(\xi_{n-1})/2 - D''(\eta_{n-1}))/D'(0)}. \tag{A.4}$$

In (A.4), we use the fact that $D''(0) \neq 0$ and that D' is continuous at zero to say that

$$\lim \frac{\log \rho_n}{\log \rho_{n-1}} = \lim \frac{\tau_n}{\tau_{n-1}} = \lim \frac{D(\tau_{n-1}) - 0}{\tau_{n-1} - 0} = D'(0) < 1. \tag{A.5}$$

From equation (A.1) and by the ratio criterion, this series is convergent.

Let d be the real number in (A.1). From (A.5), it follows that by further increasing N, for all $n \geqslant N$, we have $|\log \rho_n| \leqslant Ad^n$ for some positive A; thus, the series (A.3) is absolutely uniformly convergent, because for all $n \geqslant N$ it is bounded by a convergent geometric series, and all terms are uniformly bounded for $n \leqslant N - 1$. Thus, the series converges to a continuous function. Now, if τ_n is a point where D'' is continuous and D' is continuous at τ_n, $D^{-1}(\tau_n)$, $D^{-2}(\tau_n)$, $\ldots$, τ_0:

$$\frac{\mathrm{d}}{\mathrm{d}\tau_0} \log \rho_n = \left(\frac{\mathrm{d}}{\mathrm{d}\tau_n} \log \rho_n(\tau_n) \right) \frac{\mathrm{d}\tau_n}{\mathrm{d}\tau_0}, \qquad \text{where} \quad \frac{\mathrm{d}\tau_n}{\mathrm{d}\tau_0} = \prod_{k=0}^{n} D'(\tau_{n-k}) \tag{A.6}$$

is continuous at τ_0 and $\frac{\mathrm{d}}{\mathrm{d}\tau_n} \log \rho_n(\tau_n)$ is continuous at τ_n from equation (3.15b).

We still have to show that the series with general term (A.6) is absolutely uniformly convergent near τ_0. But this is easy because, when $n \to \infty$, from $\lim \tau_n = 0$ it follows that $\lim D''(\tau_n) = D''(0)$ and $\lim D''(\tau_n) = D''(0)$. In fact, from (A.4), since D'' is continuous at 0 and $D''(0) \neq 0$, $\lim \frac{\mathrm{d}}{\mathrm{d}\tau_n} \log \rho_n(\tau_n) = (D''(0)/2 - D''(0))/D'(0)$. Note that $\tau_{n-k} < \tau_0$ and the function D is monotone increasing, so that from (A.6) we obtain

$$\frac{\mathrm{d}\tau_n}{\mathrm{d}\tau_0} < (D'(\tau_0))^n.$$

Since $D'(\tau) < d < 1$ for $\tau \geqslant 0$, the series of the absolute values of the derivatives is uniformly bounded by a convergent geometric series. Thus the derivative is a continuous

function, represented by the series of the derivatives. Now that we know that the series is convergent, one verifies that the functional equation is satisfied. □

Remark A.2. Since $g'(0) = \lambda(0)$, taking uniformly bounded effluent particle concentration, we obtain that the corresponding solution g of the functional equation (3.20) satisfies $g'(0) < d_2$ uniformly for certain d_2. Therefore, the class of solutions $\mathcal{G}$ in theorem A.1 is not empty.

Remark A.3. Consider the functional equation (3.20) with D satisfying the hypotheses of theorem A.1. Then if D is real analytic, the corresponding solution g is real analytic.

A.2. Stability

Now we prove that our numerical solution of Julia's equation (3.20) depends continuously on the effluent concentration particle history $c_e(t)$. We consider the functions D defined on $[0, b]$ satisfying the condition (A.1). Taking $s = D(\tau)$, equation (3.9) can be rewritten as

$$g(s) = D'(D^{-1}(s))g(D^{-1}(s)). \tag{A.7}$$

We consider the effluent particle concentration $c_e(t)$ in the subset

$$\mathcal{M}_3 = \{c_e \in C^2[0, A] : 0 < r_1 < c_e(z) \leqslant r_2, c_e'(z) \neq 0\}$$

for certain constants $r_1, r_2 > 0$.

Given c_e in $\mathcal{M}_3$, the function C_e defined in (3.2*b*) depends continuously on c_e, so the following lemma holds:

Lemma A.4. *Given c_{e1}, c_{e2} in $\mathcal{M}_3$, let us define C_{e1}, C_{e2} as in (3.2b). Then the following inequality is valid:*

$$\|C_{e1} - C_{e2}\|_\infty \leqslant A\|c_{e1} - c_{e2}\|_\infty.$$

Now, we verify the validity of the following lemma.

Lemma A.5. *Given c_{e1} and c_{e2} in $\mathcal{M}_3$, let c_{i0}^1 and c_{i0}^2 be constant inlet particle concentrations such that the functions*

$$D_1(z) \equiv C_{e1}\big(z/c_{i0}^1\big), \qquad D_2(z) \equiv C_{e2}\big(z/c_{i0}^2\big) \tag{A.8}$$

satisfy condition (A.1) and denote by g_1, g_2 the solutions of equation (3.9) in $\mathcal{G}$ corresponding to D_1 and D_2 given in (A.8). Then there exist constants v_1 and v_2 that do not depend on $g_1, g_2, c_{e1}, c_{e2}, c_{i0}^1$, and c_{i0}^2, such that

$$\|g_1 - g_2\|_\infty \leqslant v_1\|c_{e1} - c_{e2}\|_\infty + v_2\big|c_{i0}^1 - c_{i0}^2\big|. \tag{A.9}$$

Proof. We use the notation

$$\|g_1 - g_2\|_\infty = \sup_{s\in[0, D^{-1}(b)]} |g_1(s) - g_2(s)|.$$

Now, using (A.7) we obtain

$$|g_1(s) - g_2(s)| = \big|D_1'\big(D_1^{-1}(s)\big)g_1\big(D_1^{-1}(s)\big) - D_2'\big(D_2^{-1}(s)\big)g_2\big(D_2^{-1}(s)\big)\big|.$$

Taking

$$N_1 = \max\{\|g_1\|_\infty, \|g_2\|_\infty\}, \qquad N_2 = \max\{\|D_1'\|_\infty, \|D_2'\|_\infty\},$$

the following inequality is valid:

$$|g_1(s) - g_2(s)| \leqslant N_1\|D_1' - D_2'\|_\infty + N_2\big|g_2\big(D_1^{-1}(s)\big) - g_2\big(D_2^{-1}(s)\big)\big|.$$

Moreover, using Taylor's formula with Lagrange's remainder we obtain

$$|g_1(s) - g_2(s)| \leqslant N_1 \|D_1' - D_2'\|_\infty + N_2 |(g_2)'(\zeta)| \left| D_1^{-1}(s) - D_2^{-1}(s) \right|,$$

where $\zeta \in \left[D_1^{-1}(s), D_2^{-1}(s) \right]$.

More generally, it is true that

$$|g_1(s) - g_2(s)| \leqslant N_1 \|D_1' - D_2'\|_\infty + N_2 |(g_2)'(\zeta)| \sup_{\tau \in [0,b]} |D_1(\tau) - D_2(\tau)|.$$

Taking $N_3 = \left(1 \big/ c_{i0}^1 c_{i0}^2\right) \max\{\|c_{e1}\|_\infty, \|c_{e2}\|_\infty\}$, we obtain $\|D_1' - D_2'\|_\infty \leqslant N_3 \left| c_{i0}^1 - c_{i0}^2 \right|$, and from lemma A.4

$$\sup_{\tau \in [0,b]} |D_1(\tau) - D_2(\tau)| \leqslant A \|c_{e1} - c_{e2}\|_\infty.$$

Finally, from theorem A.1 the solutions g of (3.9) and its derivative g' are uniformly bounded. Moreover, since c_{e1}, c_{e2} belong to $\mathcal{M}_3$ and c_{i0}^1, c_{i0}^2 are uniformly bounded, there exist constants v_1 and v_2 that do not depend on g_1, g_2, c_{e1}, c_{e2}, c_{i0}^1 and c_{i0}^2 such that inequality (A.9) holds. □

Since $\lambda = g'$, the stability of the filtration function λ with respect to c_e and c_{i0} depends on the stability estimates for the differentiation process. It is well known that the problem of numerical differentiation is ill-posed, in the sense that small perturbations of the function to be differentiated may lead to large errors in the derivative computed. In [16, 17], there are stability results and practical recommendations on stable differentiation under the assumption that the second derivative of the function to be differentiated is continuous. Thus, we can apply these results taking $c_e \in C^2$ such that the solution g of Julia's equation belongs to C^2 (see [12]).

Now, we obtain a stability estimate for the filtration function with respect to the effluent and inlet concentrations c_e and c_{i0} assuming that the differentiation process is well-posed in Tikhonov's sense (see [19, 20]): we use the fact that the differentiation process is equivalent to solving the integral equation of the first kind

$$g(\tau) = \mathcal{A}(\lambda)(\tau) = \int_0^\tau \lambda(s)\, \mathrm{d}s.$$

To obtain the Tikhonov solution, it is necessary to restrict the operator $\mathcal{A}$ to an appropriate class of functions that guarantees existence, uniqueness and stability. In [20], it is shown that, by restricting the operator $\mathcal{A} : X \to Y$ to some bounded subset $S \subset H^1[0, r]$, the differentiation operation becomes continuous in $\mathcal{A}(S)$. The proof consists of a straightforward application of the following lemmas:

Lemma A.6. *Any bounded subset of $H^1[0, r]$ is sequentially compact in the Banach spaces $C[0, r]$, i.e., spaces of continuous functions with the uniform norm.*

Lemma A.7. *The limit in $C[0, r]$ of any sequence of functions that is uniformly bounded in $H^1[0, r]$ is in $H^1[0, r]$.*

Lemma A.8. *For any bounded set $S \subset H^1[0, r]$, the operation of differentiation is continuous in $L^2[0, r]$ on the set $\mathcal{A}(S)$.*

Under the same hypotheses as in lemma A.5 and taking $S = \{\lambda \in C^1[0, r] : \|\lambda\|_\infty \leqslant k_1\}$, for some positive constant k_1, we obtain that there exists a constant v_3 that does not depend on $\lambda_1 = g_1'$ and $\lambda_2 = g_2'$ such that $\|\lambda_1 - \lambda_2\|_{H^1[0,1]} \leqslant v_3 \|g_1 - g_2\|_\infty$. Finally, applying lemma A.5 we obtain that

$$\|\lambda_1 - \lambda_2\|_{H^1[0,1]} \leqslant v_3 v_1 \|c_{e1} - c_{e2}\|_\infty + v_3 v_2 \left| c_{i0}^1 - c_{i0}^2 \right|.$$

References

[1] Alvarez A C 2004 Inverse problems for deep bed filtration in porous media *PhD Thesis* IMPA, Brazil

[2] Bedrikovetsky P G, Marchesin D, Hime G, Siqueira A G, Serra A L, Rodriguez J R P, Marchesin A O and Vinicius M 2004 Inverse problem for treatment of laboratory data on injectivity impairment *Int. Symp. and Exhibition on Formation Damage Control* (*Society of Petroleum Engineers*) SPE 86523

[3] Bedrikovetsky P G, Marchesin D, Shecaira F, Serra A L and Resende E 2001 Characterization of deep bed filtration system from laboratory pressure drop measurements *J. Petrol. Sci. Eng.* **64** 167–77

[4] Bedrikovetsky P G, Marchesin D, Shecaira F S, Serra A L, Marchesin A O, Resende E and Hime G 2001 Well impairment during sea/produced water flooding: treatment of laboratory data *SPE Latin American and Caribbean Petroleum Engineering Conf.*

[5] Bui D D and Nelson P 1992 Existence and uniqueness of an inverse problem for a hyperbolic system of lidar probing *Inverse Problems* **5** 821–9

[6] Courant R and Hilbert D 1962 *Methods of Mathematical Physics* vol II (New York: Wiley)

[7] Espedal M S, Fasano A and Mikelic A 1981 Filtration in porous media and industrial application *Lecture Notes in Mathematics* vol 1734 (Berlin: Springer)

[8] Herzig J P, Leclerc D M and Goff P Le 1970 Flow of suspensions through porous media-application to deep filtration *Indust. Eng. Chem.* **65** 8–35

[9] Iwasaki T 1937 Some notes on sand filtration *J. Am. Water Works Assoc.* **29** 1591–602

[10] John F 1982 *Partial Differential Equations* (Berlin: Springer)

[11] Kuczma M 1968 *Functional Equations in a Single Variable* (Warsaw: Polish Scientific Publishers)

[12] Kuczma M, Choczewski B and Roman G 1990 *Iterative Functional Equations* (Cambridge: Cambridge University Press)

[13] Kuhnen F, Barmettler K, Bhattacharjee S, Elimelech M and Kretzschmar R 2000 Transport of iron oxide colloids in packed quartz sand media: monolayer and multilayer deposition *J. Colloid Interface Sci.* **231** 32–41

[14] Logan D J 2001 *Transport Modeling in Hydrogeochemical Systems* (Berlin: Springer)

[15] Pang S and Sharma M M 1994 A model for predicting injectivity decline in water injection wells *69th Annual Technical Conference and Exhibition (New Orleans, Society of Petroleum Engineers)* SPE 28489

[16] Ramm A G 2001 On stable numerical differentiation *Math. Comput.* **70** 1131–53

[17] Reinsch C H 1967 Smoothing by spline functions *Numer. Math.* **10** 177–83

[18] Wennberg K I and Sharma M M 1997 Determination of the filtration coefficient and the transition time for water injection wells *Society of Petroleum Engineers* SPE 38181

[19] Tikhonov A N and Arsenin V Y 1977 *Solutions of Ill-Posed Problems* (New York: Wiley)

[20] Cullum J 1971 Numerical differentiation and regularization *SIAM J. Numer. Anal.* **8** 337–44